JOURNAL OF CATALYSIS 154, 80–90 (1995)

Selective Activation of C—H and C=C Bonds on Metal Carbides: A Comparison of Reactions of *n*-Butane and 1,3-Butadiene on Vanadium Carbide Films on V(110)

J. G. Chen

Corporate Research Laboratories, Exxon Research and Engineering Company, Annandale, New Jersey 08801

Received June 1, 1994; revised December 19, 1994

We have investigated the adsorption and decomposition of *n*-butane and 1,3-butadiene on clean and carbide-modified vanadium (110) surfaces. By using high-resolution electron energy loss spectroscopy and thermal desorption spectrometry, we observe that the formation of carbide significantly modifies the reactivities of vanadium. The 1,3-butadiene molecules interact strongly with clean V(110) via the interaction between the *d*-band of vanadium and the π orbitals of the adsorbates; the interaction is much weaker on the carbide-modified surfaces. On the other hand, *n*-butane interacts very weakly and reversibly with the clean surface; the reactivity is enhanced on carbide-modified surfaces. These experimental results are compared to the existing theories on the activation of C—H bonds of alkanes and C=C bonds of unsaturated hydrocarbons on transition metals. Such a comparison indicates that, although the reactivities of clean vanadium agree very well with the theoretical predictions for early transition metals, the properties of carbide-modified surfaces are more similar to those of Group VIIIB metals.

1. INTRODUCTION

The electronic, structural, and catalytic properties of carbides of early transition metals have been the subject of many experimental and theoretical investigations (1–3) since these carbides often demonstrate unique catalytic advantages over their parent metals in activity, selectivity, and resistance to poisoning. Among the early transition metal carbides, the electronic and catalytic properties of tungsten carbide (WC) is by far the most extensively investigated (2). Most of these studies were inspired by the pioneering work of Levy and Boudart (4), who suggested that WC displayed Pt-like behavior in several catalytic reactions. Subsequent investigations on the electronic properties have revealed many similarities and differences between WC and Pt. For example, Bennett *et al.* (5) and Colton *et al.* (6) have investigated the electronic structures of WC, up to the Fermi level, by using X-ray photoelectron spectroscopy (XPS). By comparing the valence bands and core levels of W, WC, and Pt, these authors found that WC resembled Pt more than it did W. Houston *et al.* (7) have measured the density of states (DOS) of the unfilled electronic states in the conduction bands of these three materials. They found that the width of the unfilled portion of the *d*-band of W was broadened by the formation of WC. From these studies, there is a general agreement that the electronic structure of WC is similar to that of Pt up to the Fermi level. Above the Fermi level, there is a greater density of empty levels for WC than Pt. Furthermore, the electronic structures of other early transition metal carbides are generally believed to be similar to those of WC (2, 8).

In an attempt to understand the fundamental correlations between the electronic and catalytic properties of carbide materials, we have chosen vanadium carbide films, produced on a vanadium (110) surface, as model systems for our experimental investigations. This paper is the fourth in a series of papers which discuss the possibility that the electronic modifications, resulting from the formation of metal–carbon bonds, are most likely responsible for some of the unique properties of the carbide surfaces. In the first paper (9), we have observed that the electronic properties of vanadium surfaces were significantly modified by the formation of carbide. For example, by using carbon monoxide and ethylene as probing molecules, we have observed a similarity between the surface reactivities of carbide-modified V(110) and those of platinum-group metals (9). This electronic modification effect is also supported by our near-edge X-ray absorption fine structure (NEXAFS) investigations (10), which indicate that there is a substantial charge transfer from vanadium to carbon as a result of carbide formation. In the third paper, the electronic and catalytic properties of VC/V(110) model systems were compared to those of VC powder materials (11).

In the present paper, we report our experimental results on the activation of C—H bonds of *n*-butane and C=C bonds of 1,3-butadiene on clean and carbide-modified V(110) surfaces. These two molecules are chosen because

0021-9517/95 $6.00

their carbon atoms are completely sp^3 and sp^2 hybridized, respectively. By comparing the adsorption and decomposition of *n*-butane and 1,3-butadiene, we find that the reactivities of vanadium toward these two molecules are significantly modified by the formation of carbide, although in the *opposite* directions. These results will be explained by the modification of the electronic properties of vanadium as a result of carbide formation. In addition, these results will be compared to recent theoretical investigations of C—H and C=C bond activations on transition metal surfaces (12–17).

2. EXPERIMENTAL METHODS

The experiments reported here were carried out in an ultrahigh vacuum (UHV) chamber described previously (18). Briefly, the chamber was equipped with a high-resolution electron energy loss spectrometer (HREELS) for vibrational analysis and a quadrupole mass spectrometer for thermal desorption sepctrometry (TDS) measurements. The HREELS spectra were collected in the specular direction with an incident energy of 3.5 eV and with a spectroscopic resolution of 50–80 cm^{-1}. The TDS data were obtained by simultaneously monitoring up to 16 masses, with a typical heating rate of about 1.5 K/s.

The V(110) surface was cleaned by repeated cycles of Ne^+ sputtering at 600 K (1.0 kV; 3 μA) followed by annealing to 1200–1400 K, as described in detail elsewhere (19). The impurity levels of residual C and S were less than 2 and 1%, respectively, based on Auger electron spectroscopic (AES) measurements. The residual O impurity on the surface was estimated to be less than 6% of a monolayer (ML) from the HREELS measurement (19). Thin vanadium carbide films, with an Auger C(KLL) lineshape characteristic of carbidic species(10), were produced by exposing the clean V(110) surface to ethylene or 1,3-butadiene at 600 K. At hydrocarbon exposures above 140 L (1 L = 1 × 10^6 Torr · s), the atomic ratio of carbon/vanadium reaches a constant value of 1.0, indicting a stoichiometry of VC for the thin carbide films (10). Based on the escape depth of Auger electrons from the C(KLL) and V(LMM) transitions (10, 20), the average thickness of these vanadium carbide films was estimated to be at least 10 Å. Low energy electron diffraction (LEED) measurements of these thin carbide films did not show any distinct symmetry patterns, suggesting the formation of polycrystalline carbide layers. Other carbide-modified V(110) surfaces, with the carbon/vanadium atomic ratios of less than 1.0, could be reproducibly prepared either by controlling the hydrocarbon exposures at 600 K or by heating a saturated vanadium carbide film to higher temperatures (700–1050 K) (21). For the carbide-modified V(110) surfaces used in the current study, saturated carbide films with the VC stoichiometry were prepared by exposing 300 L of deuterated 1,3-butadiene (C_4D_6) to V(110) at 600 K; carbide-modified V(110) surfaces with carbon/vanadium ratios of less than 1.0 were prepared by heating the saturated carbide films to higher temperatures. Details concerning the formation and thermal stability of thin carbide films on V(110) can be found elsewhere (21).

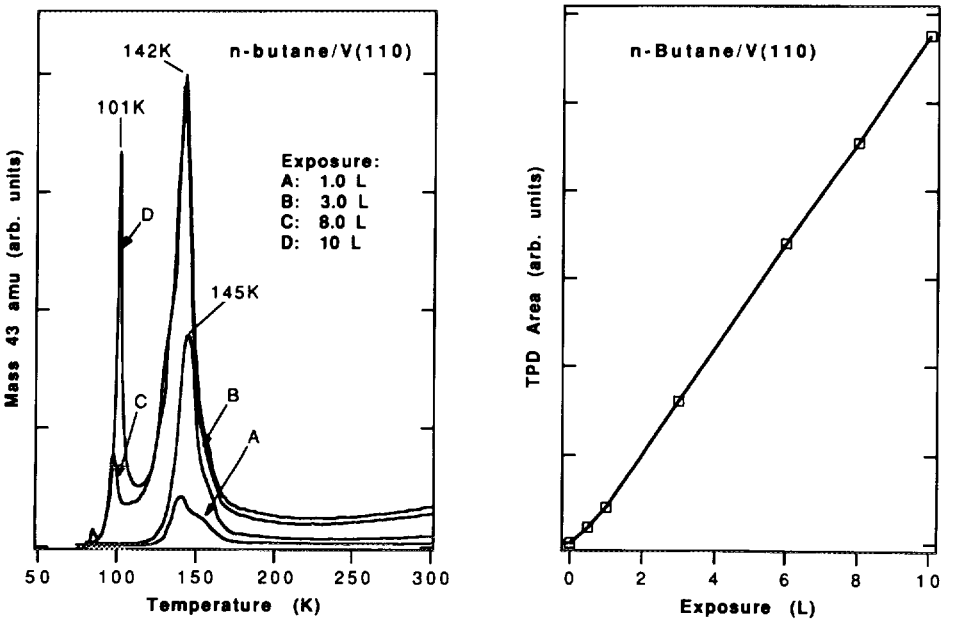

FIG. 1. TDS data of *n*-butane from the clean V(110) surface as a function of *n*-butane exposure at 80 K. The TDS spectra, shown in the left panel, were recorded by following the ion current of the major cracking pattern for *n*-butane at mass 43 amu. The right panel shows TDS peak areas of mass 43 amu at different *n*-butane exposures. The heating rate was 1.5 K/s.

Research purity reagents, *n*-butane (99.9%) and 1,3-butadiene (99.8%), were purchased from Matheson Gas Products. Deuterated 1,3-butadiene (98% atomic D) was purchased from the Cambridge Isotope Laboratory. All reagents were used without further purification and were introduced into the UHV chamber through leak-valves. The gas pressure was measured by uncorrected ion gauges.

3. RESULTS AND INTERPRETATIONS

3.1. Thermal Desorption Studies of C4 Molecules on V(110) and VC/V(110)

A set of thermal desorption spectra following the molecular desorption of *n*-butane from a clean V(110) surface is shown in the left panel of Fig. 1. The TDS results are presented by plotting the ion current of the major cracking pattern of *n*-butane at 43 amu as a function of temperature. Two peaks are detected in the TDS spectra, one at 142–145 K at low *n*-butane exposures and the other at 101 K at exposures above 8.0 L. These two TDS features can be readily assigned to the desorption of monolayer and multilayer species, respectively. A more detailed comparison of the TDS spectra (not shown) as a function of exposure suggests that multilayer formation, as indicated by the onset of the 101 K peak, occurs between an *n*-butane exposure range of 6.0–8.0 L. By using the Redhead equation for a first-order desorption process (22) and by assuming a preexponential factor of 10^{13} s^{-1}, the heats of desorption for the multilayer and monolayer coverages are estimated, from the TDS peak temperatures, to be 6.6 and 9.4 kcal/mol, respectively. Both values are in the energy range that is typically observed for physisorbed species, indicating a very weak interaction between *n*-butane and the clean V(110) surface. A weak interaction of *n*-butane with V(110) is also suggested by the peak area analysis shown in the right panel of Fig. 1, where the overall TDS peak areas (sum of monolayer and multilayer) are plotted as a function of *n*-butane exposure at 80 K. The important observation is that the peak area of molecularly desorbed *n*-butane scales almost linearly with the exposure. Assuming the sticking coefficient of *n*-butane is constant at 80 K, this observation suggests that all adsorbed *n*-butane molecules desorb molecularly from the V(110) surface without undergoing any significant amount of decomposition.

A set of TDS results following the molecular desorption of 1,3-butadiene from a clean V(110) surface is shown in Fig. 2 by monitoring the ion signals of the major cracking pattern at 39 amu. There is almost no molecular desorption from 1,3-butadiene exposures below 2.0 L (TDS spectra A and B), indicating that most of the adsorbed molecules undergo irreversible decomposition on the surface. The only detectable decomposition products of 1,3-butadiene on V(110) are atomic carbon and molecular hydrogen. The latter is produced by the recombination of atomic hydrogen and is detected from the TDS measurements at approximately 400 K, as will be discussed later. The fraction of 1,3-butadiene molecules undergoing decompo-

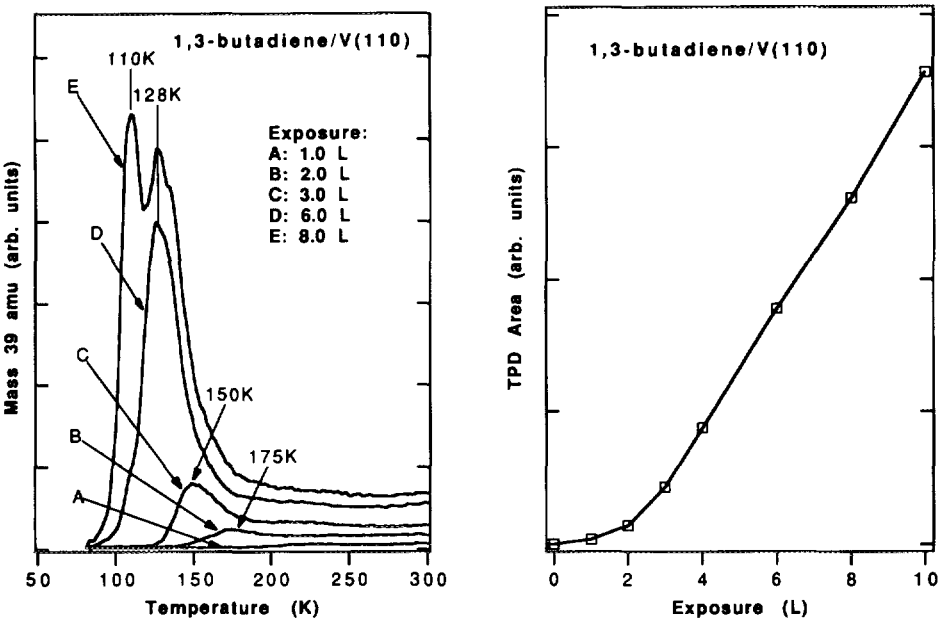

FIG. 2. TDS data of 1,3-butadiene from the clean V(110) surface as a function of exposure at 80 K. The TDS spectra, shown in the left panel, were recorded by following the ion current of the major cracking pattern for 1,3-butadiene at a mass of 39 amu. The right panel shows TDS peak areas of mass 39 amu at different 1,3-butadiene exposures.

sition reaches a constant level at exposures below 3.0 L, as suggested from the AES measurement of the concentration of atomic carbon and from the TDS measurement of the peak area of molecular hydrogen. As shown in Fig. 2, at higher 1,3-butadiene exposures (3.0–6.0 L), a desorption peak was observed at about 150 K, which shifted gradually to 128 K. An additional peak, due to multilayer desorption, was observed at 110 K at an 1,3-butadiene exposure of 8.0 L. The exposure for a saturation coverage is again estimated to be between 6.0–8.0 L. The decomposition of 1,3-butadiene at low coverages is also suggested in the peak area measurements, as shown in the right panel of Fig. 2. The lack of a linear correlation at the low exposure regime clearly indicates the irreversible nature of 1,3-butadiene adsorption at low coverages.

The TDS spectra of *n*-butane and 1,3-butadiene from carbide-modified V(110) are very different, as shown in Figs. 3 and 4. For each set of TDS experiments, the clean and carbon-modified V(110) surfaces were exposed to identical exposures of the corresponding C4 molecule at 80 K. For each set of TDS data, desorption peaks from the parent molecules and the decomposition product (hydrogen) are compared.

As shown in Fig. 3, the adsorption of *n*-butane on clean V(110) is completely reversible, as indicated by the absence of any H_2 desorption peak. On the carbide-modified surfaces, the peak area of molecularly desorbed *n*-butane decreases, which is accompanied by an increase in the peak area of H_2 at approximately 500 K. Both observations indicate that the fraction of molecules undergoing decomposition is increased on the carbide-modified surfaces.

Figure 4 shows the TDS results of 1,3-butadiene from clean and carbide-modified V(110). In contrast to those observed for *n*-butane, the fraction of 1,3-butadiene molecules undergoing decomposition is reduced on the carbide-modified surfaces, indicating that the reactivities of vanadium towards saturated and unsaturated C4 molecules are modified in a *distinctly different manner.*

We have estiimated the fraction of decomposition from the areas of the H_2-desorption peak using a combination of AES and TDS. The fraction of *n*-butane decomposition is estimated to increase from 0.01 ML on clean V(110) to 0.07 ML on the VC/V(110) surface (Fig. 3). Similarly, the fraction of 1,3-butadiene decomposition is estimated to decrease from 0.18 ML on clean V(110) to 0.04 ML on the VC/V(110) surface (Fig. 4).

3.2. Vibrational Studies of Adsorption and Decomposition of C4 Molecules

A set of HREELS spectra following the adsorption of *n*-butane on clean V(110) at 80 K is shown in Fig. 5. The two vibrational features of the "clean" surface (Fig. 6a) at 475 and 615 cm^{-1} are related to the deformation and stretching of the V–O vibrations of the residual oxygen impurities, respectively (19). Although the amount of oxygen is small, less than 0.06 monolayer (19), their vibrational features are fairly intense due to the relatively strong dynamic dipole of the V–O vibrations. The vibra-

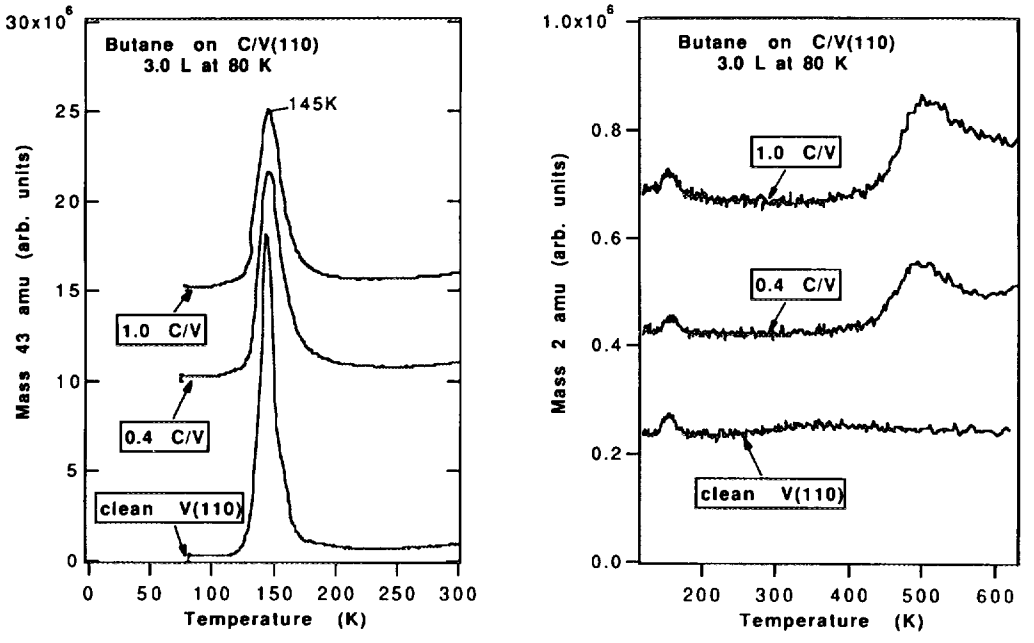

FIG. 3. TPD of H_2 are *n*-butane from carbide-modified V(110). Comparison of TDS spectra of 3.0 L *n*-butane from clean and carbide-modified V(110). The VC/V(110) surface with a C/V ratio of 1.0 was prepared by exposing the surface to 300 L of C_4D_6 at 600 K. The carbide-modified V(110) and a C/V ratio of 0.4 was obtained by annealing the 300 L C_4D_6 layer to 850 K.

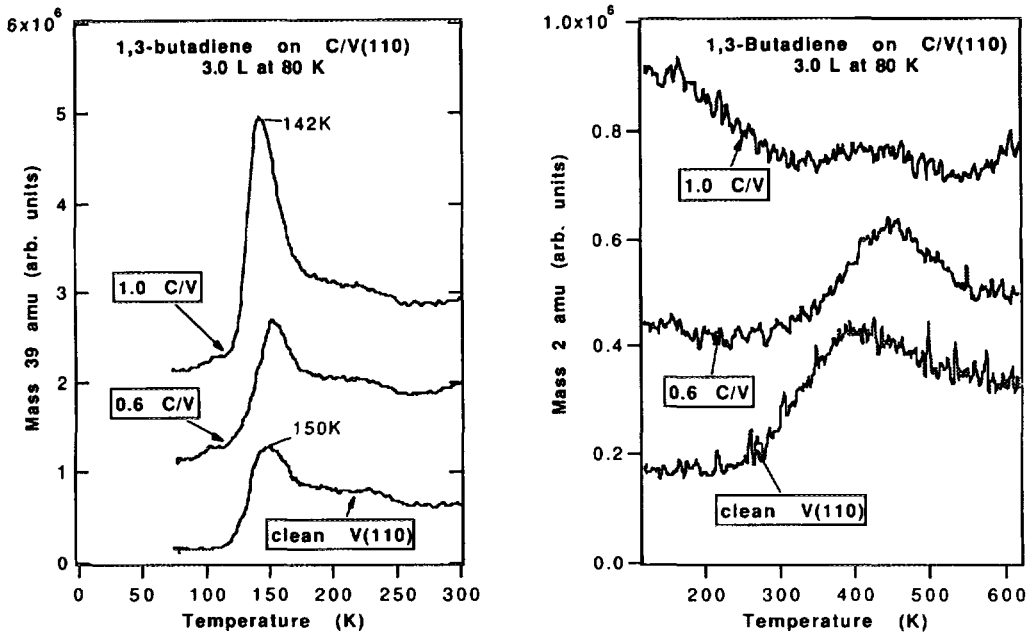

FIG. 4. TPD of H_2 and 1,3-butadiene from carbide modified V(110). Comparison of TDS spectra of 3.0 L 1,3-butadiene from clean and carbide-modified V(110). The carbide-modified surfaces were prepared in a similar way as described in Fig. 3, except that the 0.6 C/V layer was prepared by annealing the 300 L C_4D_6 layer to 750 K.

tional features of the adsorbed *n*-butane molecules can be readily assigned by a comparison with the vibrational frequencies of solid *n*-butane (23) and physisorbed *n*-butane multilayers (24): $\nu(CH_3)$ + $\nu(CH_2)$ at 2915 cm^{-1}, $\delta(CH_3)$ + $\delta(CH_2)$ at 1445 cm^{-1}, and $\nu(CC)$ at 1015 cm^{-1}.

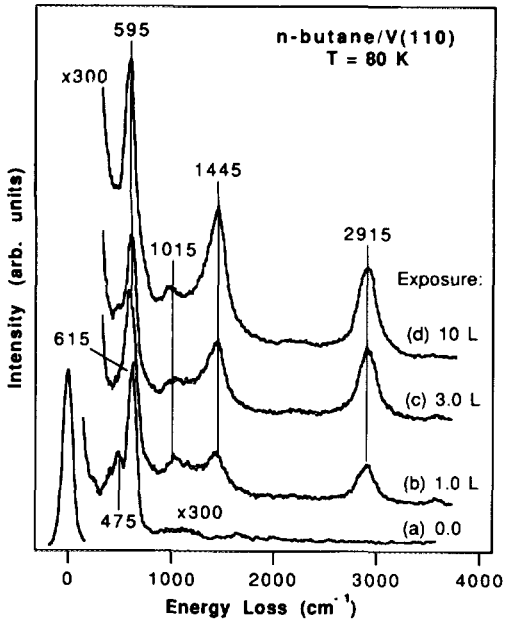

FIG. 5. HREELS spectra following the adsorption of *n*-butane on clean V(110) at 80 K. A identical set of vibrational features is observed for both submonolayer (spectra band c) and multilayer (spectrum d) coverages.

The frequencies of these features remain fairly constant as the coverage increases from submonolayer (spectra b and c) to multilayer (spectrum d), suggesting a relatively weak interaction between the adsorbate and the V(110) surface. This observation is consistent with the TDS findings of weak and reversible interaction of *n*-butane with the clean surface.

A comparison of HREELS spectra following the thermal desorption/decomposition of *n*-butane on clean and

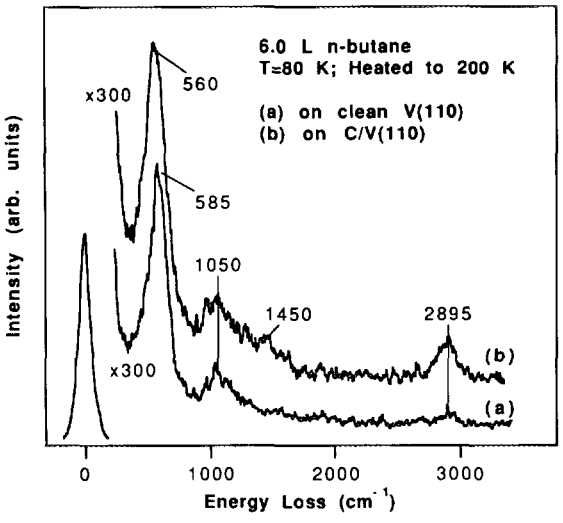

FIG. 6. A comparison of HREELS spectra following the decomposition of *n*-butane on clean V(110) and on a C/V(110) surface with an atomic C/V ratio of 0.3.

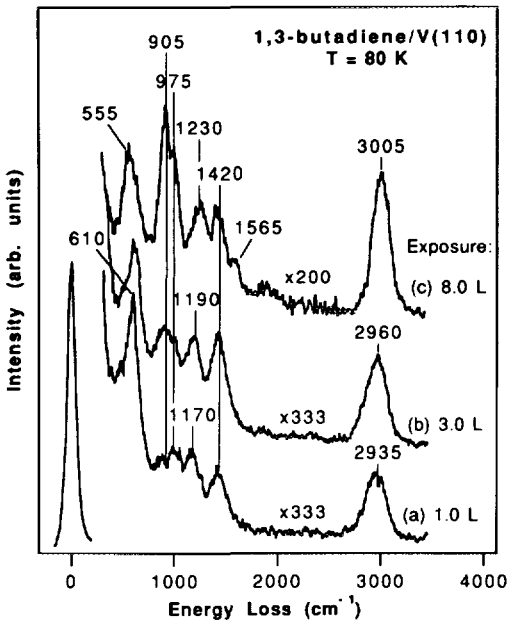

FIG. 7. HREELS spectra following the adsorption of C_4H_6 on clean V(110) at 80 K.

carbon-modified V(110) is shown in Fig. 6. The adsorbed layers were prepared by exposing the clean and carbide-modified V(110) surfaces to 6.0 L of *n*-butane at 80 K. The surfaces were then heated to 200 K, which was above the temperature for the molecular desorption of *n*-butane (Fig. 1). Therefore, the vibrational intensity of the $\nu(CH_x)$ mode in Fig. 6 can be used as a qualitative indication for the degree of *n*-butane decomposition on these two surfaces. As shown in Fig. 6a, the decomposition of *n*-butane on clean V(110) is almost negligible, as suggested by the very weak intensity of the $\nu(CH_x)$ mode at 2895 cm^{-1}. The 585 cm^{-1} feature is again related to the residual oxygen on the surface, although the peak is broader than that of the clean surface (Fig. 6a). The feature at 1050 cm^{-1} can be contributed by the accumulation of background CO (9) or hydrogen (25) during the preparation and data acquisition processes. The important observation in Fig. 7a is that the degree of *n*-butane decomposition is very small on clean V(110), which is consistent with the AES result that the carbon/vanadium atomic ratio is less than 1% after the thermal desorption of *n*-butane. By comparing Fig. 6a and 6b, one notes that the vibrational intensity of the $\nu(CH_x)$ feature at 2895 cm^{-1} is much stronger on the carbide-modified surface, indicating a larger degree of decomposition of *n*-butane on the modified surface. Although the value of x in the CH_x fragments can be distinguished by the characteristic frequencies of CH_x deformation mode in the frequency range 700–1500 cm^{-1} (26), the weak and broad features in the current study prevent us from doing so. However, the lack of a $\delta(CH)$ feature near 750 cm^{-1}, in combination with the observation of the weak 1450 cm^{-1} in spectrum b in Fig. 6, suggests that they are related to either CH_2 or CH_3 fragments. A comparison of the two HREELS spectra indicate that the amount of CH_x fragments on the carbide-modified surface is much larger than that on the clean V(110) surface. This observation is consistent with the TDS conclusions that the dissociation of *n*-butane is enhanced on the carbide-modified surfaces.

Figure 7 shows a set of HREELS spectra recorded following the adsorption of 1,3-butadiene on clean V(110) at 80 K. Unlike the case of *n*-butane adsorption on V(110) (Fig. 6), the HREELS spectra show a strong coverage dependence. The HREELS spectra at submonolayer coverages (Figs. 7a and 7b) are very different from that of the 8.0 L overlayer (Fig. 7c). For vibrational assignment, HREELS spectra following the adsorption of C_4D_6 are shown in Fig. 8. Based on the characteristic isotope shifts in the vibrational frequencies, and based on comparisons with vibrational studies of C_4H_6 adsorption on other metal surfaces (27), the vibrational features of surface species after the adsorption of 1,3-butadiene on V(110) are assigned in Tables 1 and 2.

As summarized in Table 1, at low 1,3-butadiene coverages (Figs 7a and 8a) the 1,3-butadiene species can be best described as the strongly chemisorbed tetra-σ species, VCH_2–VCH–VCH–VCH_2. In this bonding configuration, the C=C double bonds of 1,3-butadiene are reduced to C—C single bonds and all carbon atoms are in the sp^3 hybridization (27). This sp^3 environment is consistent with the observation of the characteristic vibrational frequency of the $\nu(CH) + \nu(CH_2)$ mode at 2935 cm^{-1}. The absence of any $\nu(C{=}C)$ vibrational mode, expected to appear in the frequency range 1400–1600 cm^{-1}, also supports the tetra-σ bonding configuration. HREELS results after

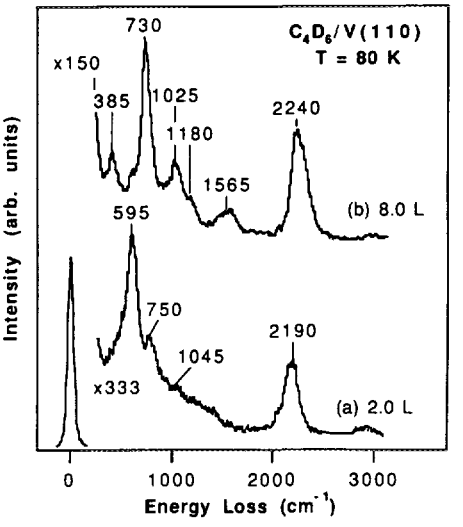

FIG. 8. HREELS spectra following the adsorption of C_4D_6 on clean V(110) at 80 K.

TABLE 1

Vibrational Assignment of tetra-σ 1,3-Butadiene Species

Vibrational modes	C_4H_6 (C_4D_6) On V(110) at Submonolayer coverage (this work)	On Pt(111) at 300 K (Ref. 27)
CH_2-Wag (out-of-plane)	975 (750)	—
ν(C–C)	1170 (—)	1050
CH_2-Scissor	1420 (1045)	1360
ν(CH) + $\nu(CH_2)$	2935 (2190)	2920

heating the low coverage 1,3-butadiene/V(110) overlayer (not shown) indicate that these strongly bonded species undergo a thermal decomposition in the temperature range 200–400 K, which is consistent with the TDS results that 1,3-butadiene adsorbs irreversibly at exposure below 2.0 L (Fig. 2).

At an 1,3-butadiene exposure of 8.0 L (Figs. 7c and 8b), the HREELS spectra are qualitatively different from those of submonolayer coverages. As indicated from the TDS data, this exposure corresponds to the completion of the first monolayer and the onset of multilayer on the V(110) surface. As summarized in Table 2, the vibrational features at this coverage can be assigned to 1,3-butadiene species adsorbed in the di-σ configuration, VCH_2—VCH—CH=CH_2. The presence of sp^2 hybridized carbon is supported by the observation of the ν(C=C) feature at 1565 cm^{-1} and the strong $\gamma(CH_2)$ mode at 905 cm^{-1}. This bonding geometry is also reflected by the vibrational frequency of ν(CH) + $\nu(CH_2)$, which shifts upward to 3005 cm^{-1}. HREELS results after heating the 8.0 L 1,3-butadiene overlayer (not shown) indicate that a tetra-σ layer is again produced on V(110) when the excess amount of 1,3-butadiene is molecularly desorbed at 150–200 K; the subsequent thermal behavior at higher temperatures is almost identical to that observed for the 2.0 L tetra-σ C_4H_6 overlayer.

Although the submonolayer C_4H_6 interacts strongly with the clean V(110) surface, as indicated by the formation of tetra-σ VCH_2–VCH–VCH–VCH_2 species, a much weaker interaction occurs on the carbide-modified V(110) surface. HREELS spectra of a submonolayer-coverage C_4H_6 on clean and on carbide-modified V(110) surfaces are compared in Fig. 9. As a reference, the HREELS spectrum of a C_4H_6 layer on an oxygen-modified V(110) surface is also shown in Fig. 9c. The vibrational frequencies observed on the O/V(110) surface are typical for the weakly adsorbed, π-bonded C_4H_6 species, with $\nu(CH_2)$ at 3045 cm^{-1}, ν(C=C) at 1590 cm^{-1}, and a very strong $\gamma(CH_2)$ mode at 935 cm^{-1}. These weakly adsorbed C_4H_6 molecules undergo a complete reversible desorption at 150 K from the O/V(110) surface. By comparing the three spectra in Fig. 9, it is clear that the bonding configuration of C_4H_6 on the carbide-modified surface (Fig. 9b) is neither tetra-σ nor π-bonded. The interaction is certainly weaker than on the clean surface, as indicated by the observation of the ν(C=C) mode at 1580 cm^{-1}. On the other hand, the spectroscopic differences between Fig. 9b and 9c suggest that the interaction is stronger than on the oxygen-modified surface. Therefore, one could conclude that the interaction of C_4H_6 with carbide-modified V(110) is between the strongly bonded tetra-σ (spectrum a) and the weakly bonded π-configurations (spectrum c). In fact, by comparing the similarities of Fig. 9b with the 8.0 L C_4H_6/V(110) spectrum (Fig. 7c), the bonding geometry of the submonolayer C_4H_6 on the carbide-modified surface is most likely in the di-σ configuations, VCH_2—VCH—CH=CH_2. This observation is consis-

TABLE 2

Vibrational Assignment of di-σ 1,3-Butadiene Species

Vibrational modes	C_4H_6 (C_4D_6) on V(110) at Monolayer coverage (this work)	On Pt(111) at 170 K (Ref. 27)
CH_2-Twist (out-of-plane)	555 (385)	570
CH_2-Wag (out-of-plane)	905 (730)	900
ν(C–C)	1230 (1180)	1050
CH_2-Scissor	1420 (1025)	1430
ν(C=C)	1565 (1565)	1400–1500
ν(CH) + $\nu(CH_2)$	3005 (2240)	2990
		3050

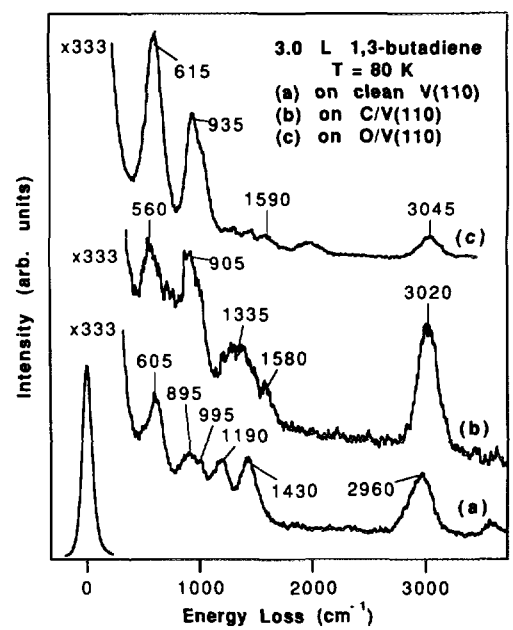

FIG. 9. A comparison of HREELS spectra following the adsorption of submonolayer 1,3-butadiene on (a) clean; (b) carbide-modified (atomic C/V = 1.0) and (c) oxygen-modified (θ_O = 0.33 monolayer) V(110) surfaces.

tent with the TDS results that the interaction of 1,3-butadiene is weaker on the carbide-modified surfaces than on the clean V(110) surface.

4. DISCUSSION

4.1. *Electronic Properties of Vanadium Carbide*

Before discussing the activation of C—H and C=C bonds on carbide-modified V(110), it is necessary to briefly review the electronic properties of vanadium carbide. As mentioned earlier, the electronic structures of early transition metal carbides are believed to be similar to those of WC (2, 8, 28). The general similarities in the electronic properties of early transition metal carbides have been demonstrated by investigating the carbon K-edge features using high-energy electron energy loss spectroscopy (EELS) (29, 30) and recently NEXAFS (31). Figure 10 shows NEXAFS results of the carbon K-edge features of the VC/V(110) films in the current study, and those of powder materials of VC, WC, and graphite. As expected, the carbon K-edge features of the three carbide materials are very different from those of graphite. All three carbides show two sharp resonances, at 285.5 and 287.5 eV for VC and at 286.8 and 289.0 eV for WC. These two resonances are characteristic for carbides materials and are related to the hybridization of C 2p and metal *d*-orbitals, as suggested from the band-structure calculations by Pfluger *et al.* (29, 30). Therefore, Fig. 10 shows that the electronic structures of VC/V(110) are almost identical to those of bulk VC powder materials, confirming that the thin VC films can be used as a reliable model system. In addition, Fig. 10 also shows the general similarities in the carbon K-edge features of VC and WC. More details about carbon K-edge features of metal carbides can be found elsewhere (10, 29–31).

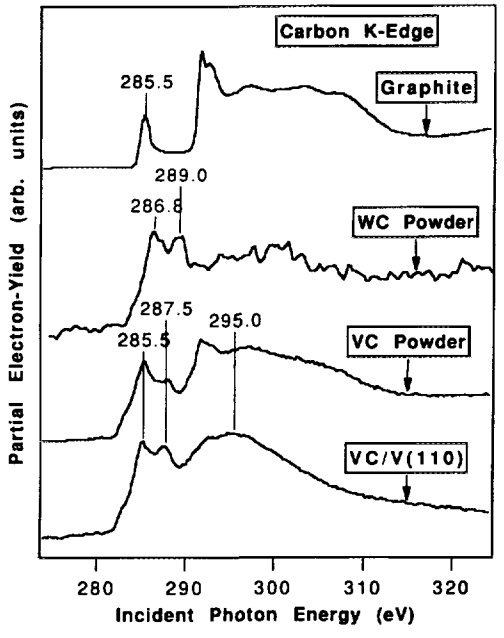

FIG. 10. A comparison of NEXAFS spectra of the VC/V(110) (twin films) model surfaces with bulk carbides. The powder materials of VC, WC, and graphite were purchased from Aldrich Chemicals.

As mentioned in the Introduction, the electronic properties of WC have been extensively investigated by various experimental techniques (4–7, 28) and theoretical calculations (32–34). By establishing the general similarities between VC and WC (Fig. 10), we will utilize the electronic structures of WC to guide our discussions in the current study. As will be discussed later, for the activation of C–H and C=C bonds, the electronic properties of both the filled and unfilled portions of *d*-bands are important factors. For WC (6–8), the filled-portion of the W *d*-band is narrowed as a result of carbide formation, resulting in the electronic structures of WC similar to that of Pt up to the Fermi level. At energies above the Fermi level, the width of the unfilled-portion of the *d*-band of W is broadened by the formation of WC, giving rise to a greater density of empty levels for WC than both W and Pt.

Finally, although the electronic properties of VC are not as extensively studied, the few investigations carried out so far confirm a similar *d*-band structures as those of WC. For example, the theoretical work of Siegel estimated that the width of the filled-portion of the V *d*-band is narrowed by at least 50% due to the formation of carbide (34). In addition, we have observed a broadening in the unfilled-portion of *d*-orbitals of VC in our NEXAFS investigations of the lineshape of the vanadium L-edge features of V and VC (11).

4.2. *Activation of C–H and C=C Bonds on V(110) and VC(110)*

The TDS and HREELS results presented here clearly demonstrate that the formation of vanadium carbide modifies the reactivities of vanadium toward *n*-butane and 1,3-butadiene. On clean V(110), the decomposition of C–H bonds of *n*-butane is negligible, as indicated by the lack of H_2-desorption in th TDS measurements (Fig. 3) and by the absence of surface CH_x fragments in the HREELS results (Fig. 6). On the other hand, the decomposition of *n*-butane is enhanced on the carbide-modified surfaces, as demonstrated by the detection of H_2-desorption in the TDS measurements (Fig. 3) and by the HREELS detection of CH_x fragments (Fig. 6).

Different modification effects are observed for the interaction of 1,3-butadiene on clean and carbide-modified V(110) surfaces. At exposures below 2.0 L, the strong interaction between the C=C bonds of 1,3-butadiene and the clean V(110) surface reduces the bond-order to C–C single bonds, as indicated by the HREELS observation

of the tetra-σ species, VCH_2–VCH–VCH–VCH_2 (Figs. 7a and 8a). These strongly bonded species decompose on the surface at higher temperatures. The decomposition products are atomic carbon and molecular hydrogen, which desorbs as a very broad TDS peak centered at 400 K. On the other hand, the interaction of 1,3-butadiene on the carbide-modified surface is weakened. For example, on a carbide-modified surface with a C/V ratio of 1.0 (Fig. 9b), the C=C bond is partially protected, as indicated by the HREELS observation of the ν(C=C) mode at 1580 cm^{-1} and the sp^2-like ν(CH) feature at 3020 cm^{-1}. The TDS results (Fig. 4) also indicate that the areas of the H_2-desorption peaks are reduced on the carbide-modified surfaces. However, it is important to point out that, although the interaction of 1,3-butadiene on vanadium carbide is weaker than that on clean V(110), there is still significant interaction between the adsorbate and the carbide surface. This is suggested by the TDS observation that H_2-desorption peak is still detected even on the vanadium carbide surface with a carbon/vanadium ratio of 1.0 (Fig. 4). This is also supported by the HREELS observation that the vibrational spectrum (Fig. 9b) is much different from the weak and reversible adsorption of 1,3-butadiene on the oxygen-modified V(110) surface (Fig. 9c). The HREELS spectrum of 1,3-butadiene on vanadium carbide (Fig. 9b) might be best described as a di-σ species, VCH_2—VCH—CH=CH_2, suggesting that there is still a relatively strong interaction between the C=C bonds of 1,3-butadiene and the VC/V(110) surface.

The differences in the reactivities of 1,3-butadiene with clean and carbide-modified V(110) surfaces can be explained by the different electronic properties of the two surfaces. The activation and subsequent decomposition of C=C bonds involve the donation of metal *d*-electrons to the antibonding $p\pi^*$-orbitals of the unsaturated hydrocarbons (12). On clean V(110), the diffuse *d*-orbitals, characteristic for early transition metals (35), would allow a very efficient d–$p\pi^*$ overlapping between the substrate and the C=C bonds of the absorbates. This is consistent with our observation of the formation of the tetra-σ VCH_2–VCH–VCH–VCH_2 species on clean V(110). As mentioned earlier, the formation of carbide narrows the filled-portion of the metal *d*-band, which would result in a less efficient d–$p\pi^*$ overlapping. This is again consistent with our observation of a weaker interaction between 1,3-butadiene and the VC/V(110) surface.

We should also point out that the reactions of unsaturated hydrocarbons (36–40) and cyclic hydrocarbons (41, 42) have also been investigated on carbon-modified single crystal surfaces of W and Mo. The main effect of carbon modification is that the presence of carbon/carbide reduces the degree of interaction between the unsaturated hydrocarbons and the surfaces (36–40). Most of these results are explained by a site-blocking model (40), which assumes that carbon atoms block those surface active sites that are interacting strongly with adsorbates. In the current study, we believe that the electronic modification on the *d*-band, instead of a pure site-blocking mechanism, plays a major role in the interaction of 1,3-butadiene with the VC/V(110) surface. For example, for the VC/V(110) surface used in Fig. 9b, the thickness of the VC film is at least 10 Å (10). The fact that a relatively strong interaction is still observed on this VC/V(110) surface, as indicated by the formation of di-σ VCH_2—VCH—CH=CH_2 species, argues against a pure site-blocking model.

The interaction of saturated hydrocarbons with carbide-modified single crystal surfaces has not been extensively investigated. To our best knowledge, the only systematic investigation was carried out by Kelly *et al.* (40), who carried out a detailed TDS investigation of the decomposition of *n*-butane on clean and on carbon-modified Mo(100). They found that the degree of *n*-butane decomposition is small and more than 95% of *n*-butane desorbs molecularly from both clean and carbide-modified surfaces. For the 5% adsorbates which react with the surface, the major decomposition product changes from hydrogen on clean Mo(100) to butene on carbide-modified surfaces with carbon coverages above 2/3 monolayer. Such a change in the decomposition pathway was again attributed to the site-blocking of carbon, which prevented the total decomposition of *n*-butane to hydrogen and atomic carbon species (40).

In the current study, the TDS and HREELS experiments clearly indicate that the decomposition of *n* butane is enhanced on carbide-modified V(110). The site-blocking model for C/Mo(110) (40) will not provide a satisfactory explanation. We propose the following three possible models for the enhancement in the decomposition of *n*-butane on VC/V(110):

(i) It might be related to the unique electronic structures of early transition metal carbides at above the Fermi level. As mentioned earlier, the unfilled-portion of the metal *d*-band is broadened after the formation of carbide. A recent study suggests that the C–H bond of alkanes can be weakened when it is bonded in the three-center, agostic bonding model (43), which involves the donation of the electron pair of the C–H bond to a vacant orbital on the metal center. The availability of the broad, unoccupied orbitals on the carbide surfaces should therefore enhance the probability for the activation of C–H bonds of alkanes. Similar interaction model has been proposed by Ohkubo *et al.* (43). In fact, Ohkubo *et al.* observed that the rate constant for ethylbenzene dehydrogenation increased with the ability of carbides to accept electrons (43).

(ii) The surface defects on the carbide-modified surfaces might play a role in the activation of the C–H bond of alkanes. However, the surface defect sites are most likely

not the only contributor to the enhanced C–H bond activation for the following reason: We have investigated the smoothness (i.e., surface reflectivity) of carbide-modified V(110) by comparing the intensities of the (0,0) beam in the HREELS measurements for V(110), VC/V(110), and for carbide-modified surfaces with C/V atomic ratios of less than 1.0 (21). We find that the relative smoothness of the surface follows the order V(110) > VC/V(110) > carbide-modified surfaces with C/V ratios of 0.3–0.8 (21). However, in our TDS measurements, we find that the degree of *n*-butane decomposition, as judged by the relative intensity of the H_2-desorption peak, increases gradually with the C/V atomic ratios of the carbide-modified surfaces. More control-experiments will be needed to quantify the role of the defect sites.

(iii) The enhanced C–H bond activation might also be related to the similarities in the electronic properties of VC/V(110) to group VIIIB metals, which will be the subject of the next section.

4.3. Comparison with Theories of C–H and C=C Bonds Activation

The activation mechanisms of C=C bonds of alkenes and C–H bonds of alkanes on transition metals have been the subject of several recent theoretical papers (12–15). For example, decomposition mechanisms of the C=C bond of ethylene (12) and C–H bonds of methane (13) have been proposed for the entire second-row transition metals, and trends in the reactivities from the left side to the right side of the Periodic Table have been observed.

In brief, as pointed by Blomberg *et al.* (13), the energetic barrier for the decomposition of C–H bonds on transition metal surfaces is primarily determined by two factors. The first one requires the least amount of repulsive force when the C–H group approaches the metal; the least repulsive state of the metal is the $d^{n+2}s^0$ configuration. The second factor is related to the energies gained as a result of the formation of two covalent bonds of *M*–H and *M*–CH_3; the lowest lying state that can form two covalent bonds is the $d^{n+1}s^1$ configuration. By comparing the promotion energies for various transition metals, Blomberg *et al.* predict that, for the activation of C–H bonds of alkanes, Group VIIIB metals would be much more efficient than the early transition metals (13). This is in agreement with experimental studies on transition metal surfaces, where an appreciable amount of decomposition of light alkanes are generally observed on Group VIIIB metals. For example, the dissociative adsorption of normal alkanes (C2–C7), under ultrahigh vacuum (UHV) conditions, has been reported on single crystal surfaces of Ir(110)–(1 × 2) (45–47), Pt(110)–(1 × 2) (48), and on thin films of Pt (49). Our experimental results also agree well with these theoretical predictions concerning the activation of C–H bonds. As expected for early transition metals, the decomposition of *n*-butane is negligible on the clean V(110) surface. Furthermore, the enhancement of *n*-butane decomposition on VC/V(110) might also be explained by the argument that the electronic properties of vanadium carbide are similar to those of Group VIIIB metals.

For the interaction of C=C bonds of unsaturated hydrocarbons with transition metals, Blomberg *et al.* (12) have proposed several types of bonding configurations between the C=C bond and the metal atom, depending on the location of the metal in the Periodic Table. For those metals on the left side of the Periodic Table (Groups IIIB to VB), a covalent bond is predicted between ethylene and metal atoms, which effectively reduces the C=C double bond to a C–C single bond. For those metals on the right side of the Periodic Table (Group VIIIB), the bonding is considered to be a compromise between the covalent and donation–back–donation forms of bonding (12), giving rise to a carbon–carbon bond order roughly in between that of a double and a single bond. Again, our experimental results of 1,3-butadiene on V(110) and VC/V(110) agree well with these theoretical predictions. As expected for early transition metals, the observation of the tetra-σ species, VCH_2–VCH–VCH–VCH_2, on clean V(110) confirms the very strong interaction between the C=C bonds of 1,3-butadiene and the surface. The reactivity of the VC/V(110) surface again compares favorably to those of Group VIIIB metals, as indicated by the formation of the di-σ species (VCH_2–VCH–CH=CH_2), with only one of the two C=C bonds being reduced to a C–C single bond. In fact, the di-σ species was found to be the major surface species after the adsorption of 1,3-butadiene on Pt(111) at 170 K (27), further supporting the similarities of VC/V(110) and Group VIIIB metals.

5. CONCLUSIONS

From the results and discussion presented above, we summarize the following important observations for the reactions of *n*-butane and 1,3-butadiene on clean and on carbide-modified V(110) surfaces:

(i) On clean V(110), 1,3-butadiene interacts strongly via an overlapping of the *d*-bands of vanadium and π-orbital of the C=C bonds of adsorbates. However, *n*-butane interacts only very weakly with the clean surface at 80 K and desorbs molecularly at 142 K.

(ii) On carbide-modified V(110), the decomposition of 1,3-butadiene is reduced, although not completely inhibited. On the other hand, the dissociation of *n*-butane is enhanced on the vanadium carbide surfaces.

(iii) The experimental results are compared to theoretical investigation (12–15) concerning the activation mecha-

nisms for C–H and C=C bonds on transition metals. Such a comparison indicates that, although the reactivities of clean V(110) agree very well with the theoretical predictions for early transition metals, the properties of carbide-modified V(110) surfaces are similar to those of Group VIIIB metals.

(iv) We believe that the modified reactivities of vanadium carbides are most likely related to a modification of the electronic structures as a result of V–C bond formation. The previously proposed site-blocking model (40) could also contribute to some of the observed reactivities.

ACKNOWLEDGMENTS

We acknowledge Drs. J. M. White, Z.-M. Liu, M. L. Colaianni, and M. S. Touvelle for helpful discussion.

REFERENCES

1. Tontegode, A. Ya., *Prog. Surf. Sci.* **38,** 201 (1991), and references therein.
2. Oyama, S. T., and Haller, G. L., *in* "Catalysis" (Specialist Periodical Reports), Vol. 5, p. 333. Royal Chem. Soc., London, 1982, and references therein.
3. Iglesia, E., Ribeiro, F. H., Boudart, M., and Baumgartner, J. E., *Catal. Today* **15,** 307 (1992).
4. Levy, R., and Boudart, M., *Science* **181,** 547 (1973).
5. Bennett, L. H., Cuthill, J. R., McAlister, A. J., Erickson, N. E., and Watson, R. E., *Science* **184,** 563 (1974).
6. Colton, R. J., Huang, J. J., and Rabalais, J. W., *Chem. Phys. Lett.* **34,** 337 (1975).
7. Houston, J. E., Laramore, G. E., and Park, R. L., *Science* **185,** 258 (1974).
8. Ramqvist, L., *J. Appl. Phys.* **42,** 2113 (1971).
9. Chen, J. G., Weisel, M. D., Liu, Z.-M., and White, J. M., *J. Am. Chem. Soc.* **115,** 8875 (1993).
10. Chen, J. G., Kim, C. M., Fruhberger, B., DeVries, B. D., and Touvelle, M. S., *Surf. Sci.*, **321,** 145 (1994).
11. Chen, J. G., Fruhberger, B., Weisel, M. D., Baumgartner, J. E., and DeVries, B. D., *in* "Transition Metal Carbides and Nitrides" (S. T. Oyama, Ed.), in press.
12. Blomberg, M. R. A., Siegbahn, P. E. M., and Svensson, M., *J. Phys. Chem.* **96,** 9794 (1992).
13. Blomberg, M. R. A., Siegbahn, P. E. M., and Svensson, M., *J. Am. Chem. Soc.* **114,** 6095 (1992), and references therein.
14. Siegbahn, P. E. M., and Blomberg, M. R. A., *J. Am. Chem. Soc.* **114,** 10,548 (1992).
15. Siegbahn, P. E. M., Blomberg, M. R. A., and Svensson, M., *J. Am Chem. Soc.* **115, 1952 (1993).**
16. Blomberg, M. R. A., Brandemark, U., Pettersson, L., and Siegbahn, P. E. M., *Int. J. Quantum Chem.* **23,** 855 (1983).
17. Blomberg, M. R. A., Siegbahn, P. E. M., Nagashima, U., and Wennerberg, J., *J. Am. Chem. Soc.* **113,** 476 (1991).
18. Hrbek, J., de Paola, R. A., and Hoffmann, F. M., *J. Chem. Phys.* **81,** 2818 (1984); Chen, J. G., Weisel, M. D., and Hall, R. B., *Surf. Sci.* **250,** 159 (1991).
19. Kim, C. M., DeVries, B. D., Fruhberger, B., and Chen, J. G., *Surf. Sci.*, in press.
20. The escape depth of Auger electrons were estimated from the universal curve in: Ertl, G., and Kuppers, J., "Low Energy Electrons and Surface Chemistry," Monographs in Modern Chemistry 4. p. 4 VCH, Weinheim/New York, 1974.
21. Chen, J. G., DeVries, B. D., Fruhberger, B., Kim, C. M., and Liu, Z.-M., *J. Vac. Sci. Technol.*, in press.
22. Redhead, P.A., *Vacuum,* **12,** 203 (1962).
23. Shimanouchi, T., "Tables of Molecular Vibrational Frequencies," Consolidated Volume I, NSRDS-NBS 39, Natl. Bur. of Standards, Washington, DC, 1972.
24. Chesters, M. A., Gardner, P., and McCash, E. M., *Surf. Sci.* **209,** 89 (1989).
25. Chen, J. G., unpublished data. (A relatively strong ν(V–H) mode was detected in the range 1065–1080 cm^{-1} after exposing V(110) to 30 L of H_2 at 80 K. Off-specular HREELS measurements indicate that this vibrational feature is excited primarily by the impact scattering mechanism.)
26. See, for example, Biener, J., Schenk, A., Winter, B., Lutterloh, C., Schubert, U. A., and Kuppers, J., *Surf. Sci. Lett.* **291,** L725 (1993).
27. Avery, N. R., and Sheppard, N., *Proc. R. Soc. London A* **405,** 27 (1986).
28. Ramqvist, L., Hamrin, K., Johansson, G., Fahlman, A., and Nordling, C., *J. Phys. Chem. Solids* **30,** 1835 (1969).
29. Pflüger, J., Fink, J., Crecelius, G., Bohnen, K. P., and Winter, H., *Solid State Commun.* **44,** 489 (1982).
30. Pflüger, J., Fink, J., and Schwarz, K., *Solid State Commun.* **55,** 675 (1985).
31. Kapoor, R., Oyama, S. T., Fruhberger, B., DeVries, B. D., and Chen, J. G., submitted for publication.
32. Ern, V., and Switendick, A. C., *Phys. Rev. A.* **137,** 1927 (1965).
33. Conklin, J. B., and Silversmith, D. J., *Int. J. Quantum Chem.* **11,** 243 (1968).
34. Siegel, R., *Semicond. Insul.* **5,** 47 (1979).
35. Kang, D. B., and Anderson, A. B., *Surf. Sci.* **165,** 221 (1986).
36. Ko, E. I., and Madix, R. J., *Surf. Sci.* **100,** L449 (1980).
37. Pearlstine, K. A., and Friend, C. M., *J. Vac. Sci. Technol. A* **2,** 1021 (1984).
38. Pearlstine, K. A., and Friend, C. M., *J. Am. Chem. Soc.* **107,** 5898 (1985).
39. Wang, L. P., and Tysoe, W. T., *J. Catal.* **128,** 320 (1991).
40. Kelly, D. G., Salmeron, M., and Somorjai, G. A., *Surf. Sci.* **175,** 465 (1986).
41. Touvelle, M. S., Ph.D. Dissertation, Department of Chemistry, Northwestern University, 1991.
42. Kellogg, D. F., Touvelle, M. S., and Stair, P. C., *J. Catal.* **120,** 192 (1989).
43. Ohkubo, K., Shimada, H., and Okada, M., *Bull. Chem. Soc. Jpn.* **45,** 3475 (1972).
44. Brookhart, M., Green, M. L. H., and Wong, L.-L., *Prog. Inorg. Chem.* **36,** 1 (1988).
45. Wittrig, T. S., Szuromi, P. D., and Weinberg, W. H., *J. Chem. Phys.* **76,** 3305 (1982).
46. Szuromi, P. D., Engstrom, J. R., and Weinberg, W. H., *J. Chem. Phys.* **80,** 508 (1984).
47. Szuromi, P. D., and Weinberg, W. H., *Surf. Sci.* **149,** 226 (1985).
48. Szuromi, P. D., Engstrom, J. R., and Weinberg, W. H., *J. Phys. Chem.* **89,** 2497 (1985).
49. Lisowski, W., and Dus, R., *Surf. Sci.* **118,** 208 (1982).